Proceedings of the
Annual Stability Conference
Structural Stability Research Council
Nashville, Tennessee, March24-27, 2015

Buckling mode identification for a cold-formed steel column experiment with 3D image-based reconstruction

AbrahamLama-Salomon[1],Fannie Tao[2], Junle Cai[3], Cristopher D.Moen[4]

Abstract

Recently developed thin-walled modal decomposition algorithms are used with 3d-image based reconstruction to document and quantify buckling deformation throughout cold-formed steel column experiments. The buckling deformation is documented with off-the-shelf digital cameras. Images are processed with a gradient-based optimization algorithm, available in low cost commercial software packages, that finds the 3d image coordinates and camera position by maximizing the number of matching (overlapping) pixels. Once the 3d coordinate system and camera locations are established, a dense point cloud is generated resulting in the 3dcolumn representation at several load stages in the experiment. The 3d point cloud is analyzed with a buckling mode identification tool that employs cross-sectional deformation modes from generalized beam theory. Local, distortional, and global buckling participation are quantified, including contributions just prior to column failure which can be useful for the development of future strength prediction design approaches, especially where buckling modes mix near an ultimate limit state.

1. Introduction

Technology to produce accurate image-based reconstruction of 3d objects is now mature (Wu 2011; Wu 2013), and it is finding its way into civil engineering applications ranging from construction management (Golparvar-Fard et al. 2009) to post-disaster building assessment (Torok et al. 2013). Image-based reconstruction is appealing because the 3d object, represented as a point cloud, can be created with off the shelf point-and-click digital still or video cameras in contrast to physical contact measurements (calipers, rulers, wire potentiometers). The research described herein brings 3d documentation and automated modal identification to structural testing in a similar way to recent work applied to collapse simulations (Zi et al. 2011). The approach is applied to thin-walled cold-formed steel structural stud in compression, creating a 3d record at several instances during the experiment, including initial geometric imperfections and buckling modes under load.

[1]Graduate Research Assistant, Civil & Environmental Engineering, Virginia Tech, <abrah89@vt.edu>
[2]Graduate Research Assistant, Civil & Environmental Engineering, Virginia Tech, <ftao1@vt.edu>
[3]Graduate Research Assistant, Civil & Environmental Engineering, Virginia Tech, <junlecai@vt.edu>
[4]Associate Professor, Civil & Environmental Engineering, Virginia Tech, <cmoen@vt.edu>

The fundamental technology supporting 3d image-based reconstruction is described in Figure 1. Digital video or images are recorded of an object or group of objects from enough locations to provide 360 degree coverage. In the realm of civil engineering, these objects could be bridge girder superstructure, concrete pavement, or a cable-stayed bridge pylon. The video is decomposed into individual frames as shown for a one-way concrete bridge deck slab test at Virginia Tech in Figure 1 (Zheng and Moen 2013), note the image frames from different angles in Figure 1a.

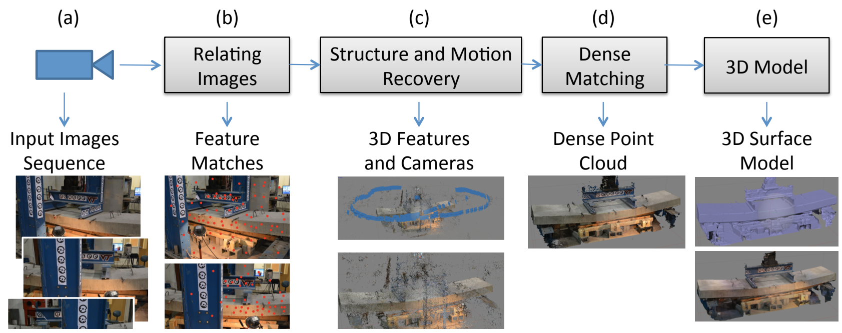

Figure 1: 3d image-based reconstruction applied to a one-way bridge deck slab test at Virginia Tech: (a) image frame collection from 360 degree perspectives; (b) relating images with feature matching using gradient-based optimization; (c) structure and motion recovery to identify camera and image location in 3d space; (d) dense 3d point cloud generation; (e) adding surface meshing and texture informed by 2d image frames

A discrete-continuous gradient-based optimization algorithm (e.g., Crandell et al. 2011) is applied that finds the 3d image coordinates and camera position by maximizing the number of matching (overlapping) features from image to image (Figure 1b). Once the 3d coordinate system and camera locations are established (Figure 1c), a dense point cloud (Figure 1d) is generated resulting in the 3d representation. This procedure sounds complicated but is robustly implemented in user-friendly, freely available open-source code, for example Structure for Motion (Wu 2011), and low cost commercial software like Agisoft PhotoScan (Perry 2013) that was used in this project.

Automated structural measurement and assessment is not new, with previous efforts in civil engineering focused on pavement evaluation (Cheng and Glazier 2002; Wang 2004). Current ongoing work using low-cost measurement equipment includes RGB-D sensors like the Microsoft Kinect have been applied to cold-formed steel framing post-blast records (Whelan et al. 2015). A major effort is ongoing to construct a database of initial geometric imperfections for cold-formed steel with a custom-built laser scanner (McAnallen et al. 2014) hosted by the Cold-Formed Steel Research Consortium.

The project described herein documents steps for applying3d image-based reconstruction to column experiments. Cold-formed steel studs with fixed-fixed boundary conditions are tested to collapse in compression. Point clouds at multiple steps in the tests are generated using digital cameras and compared to manual measurements. A generalized beam theory modal identification approach is used to deconstruct the point clouds into linear combinations of pure modes, providing insight into modal participation that can inform future design approaches. The experimental program is introduced in the next section followed by the 3d point cloud results.

2. Experimental Program

Cold-formed steel 362S162-33 Cee-section studs,890 mm long between warping fixed supports, were subjected to compression testing until failure as shown in Figure 2.Specimen 1 was marked with a grid and Specimen 2 was marked with random dots to explore different techniques for creating the image reconstructions. (A specimen without markings was also tested however the lighting was not adequate to complete the image-based reconstruction, a lesson learned that was adjusted on the following two tests presented here). Full details of the testing program, including tested capacities and load-deformation response, are detailed in Tao et al. (2015).

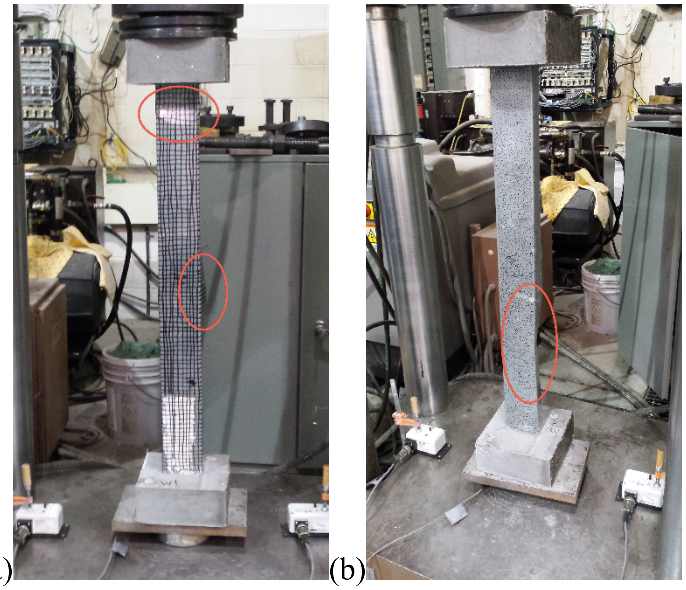

(a) (b)

Figure 2: Cold-formed steel stud column test specimens :(a) Specimen 1 with grid pattern and (b) Specimen 2 with random dots applied

For both tests, image reconstruction was performed before loading, at 22 kN of compression, 44 kN (near peak load), and then after peak load at 22 kN again. A digital single-lens reflex (DSLR) Nikon D7100 camera was used to take the specimen pictures with24 megapixels resolution. At each load step, a sequence of approximately 120 images were taken covering a 360 degree view, making sure to overlap the image frame as each picture was taken. Both specimens experienced local-global buckling with three distortional buckling half-waves forming along the column length and this deformation was captured by the imaged-based reconstruction.

3. 3d Column Image-Based Point Cloud Reconstruction

The digital images from each test were input into a commercial computer program called Agisoft PhotoScan (Perry 2013) which uses Structure From Motion (SFM) techniques (Wu 2013) to estimate the three-dimensional coordinates of a structure from two-dimensional image sequences. The results from each 3d reconstruction are shown in Figures 3 and 4.

(a) 0 kN (b) 22 kN (c) 44 kN (d) 22 kN

Figure3: 3d image-based reconstruction point clouds for Specimen 1

(a) 0 kN (b) 22 kN (c) 44 kN (d) 22 kN

Figure 4: 3d image-based reconstruction point clouds for Specimen 2

The 3D point clouds for each test, i.e., Figure 4 a-d, were aligned with each other using an Agisoft Photoscan tool matching the points in the initial dense point cloud (roughly 30,000,000 points) as shown in Figure 5.

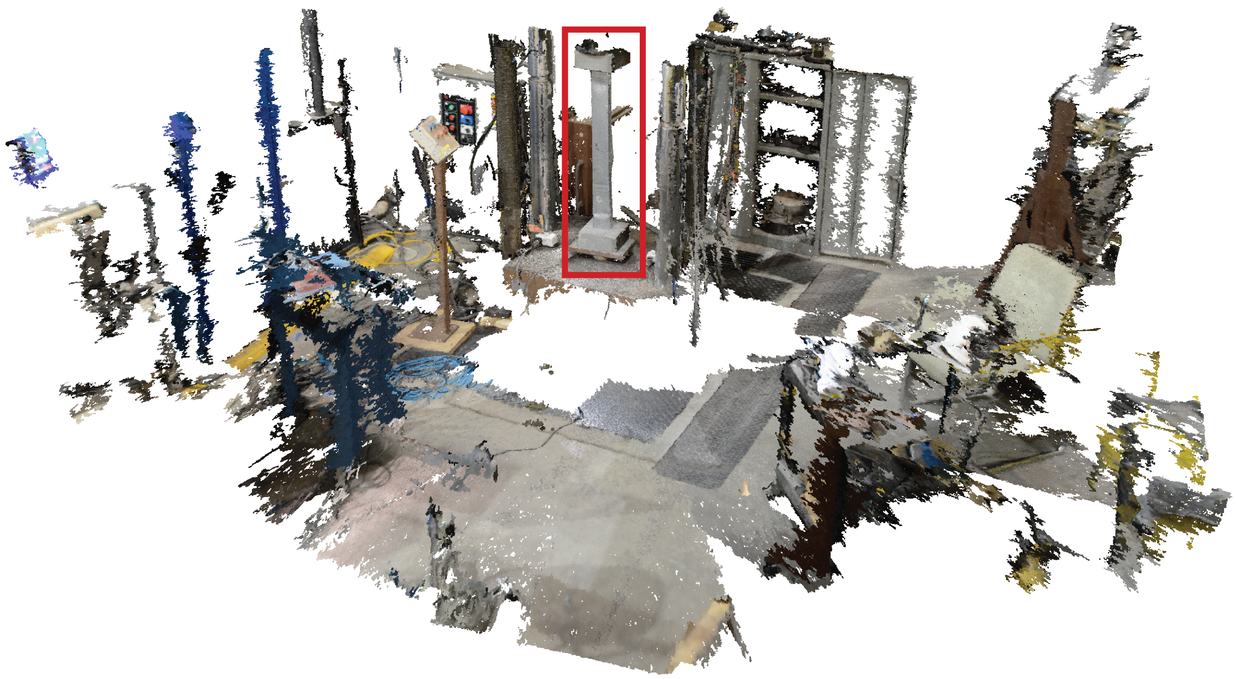

Figure 5: Raw dense point cloud, test specimen inside red rectangle (approximately 30,000,000 points)

After the initial alignment of each load step the point clouds were scaled and analyzed using custom MATLAB code. Each reconstruction was scaled so that it matched the distance between supports (e.g., 890 mm) resulting in pre-tested cross-section web dimension errors of about 1.0% when compared to manual measurements, i.e., out-to-out web was measured as 92 mm and 91 mm is measured in the 3d reconstruction.

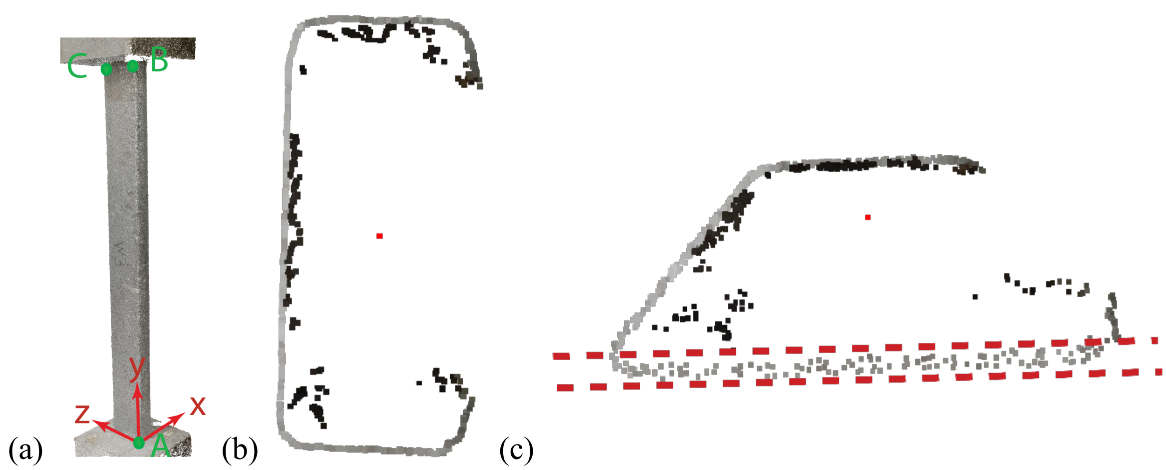

Figure 6:(a)Model axis alignment, (b) raw point cloud, (c) isometric point cloud view with 0.25 mm section cut

The *Y*-axis was aligned to the element longitudinal axis and the *Z*-axis to the web, as shown in Figure 6a. The alignment procedure was performed by selecting 3 points (i.e., A,B,C in Figure 6a), the first one at the bottom support in the section corner, the second at the top support at the section corner, and the third one at the top support in the opposite web section corner. The *X*-axis was considered as the vector perpendicular to A-B and B-C. Point cloud cross-sections, 200 evenly distributed along the length of each specimen, were obtained by grouping all the points within ±0.25 mm to a cross-section plane and compressing them to be coplanar, see Figure 6b and 6c. Point clouds at the lips are not consistent with the actual member shape because the lighting caused shadows that confused the image reconstruction algorithm.

Figure 7 highlights potential application of the 3d image-based reconstruction. Mid-height cross-section deformation for Specimen 2 is tracked, showing distortional buckling deformation of the flanges transitioning to weak axis flexural buckling after peak load.

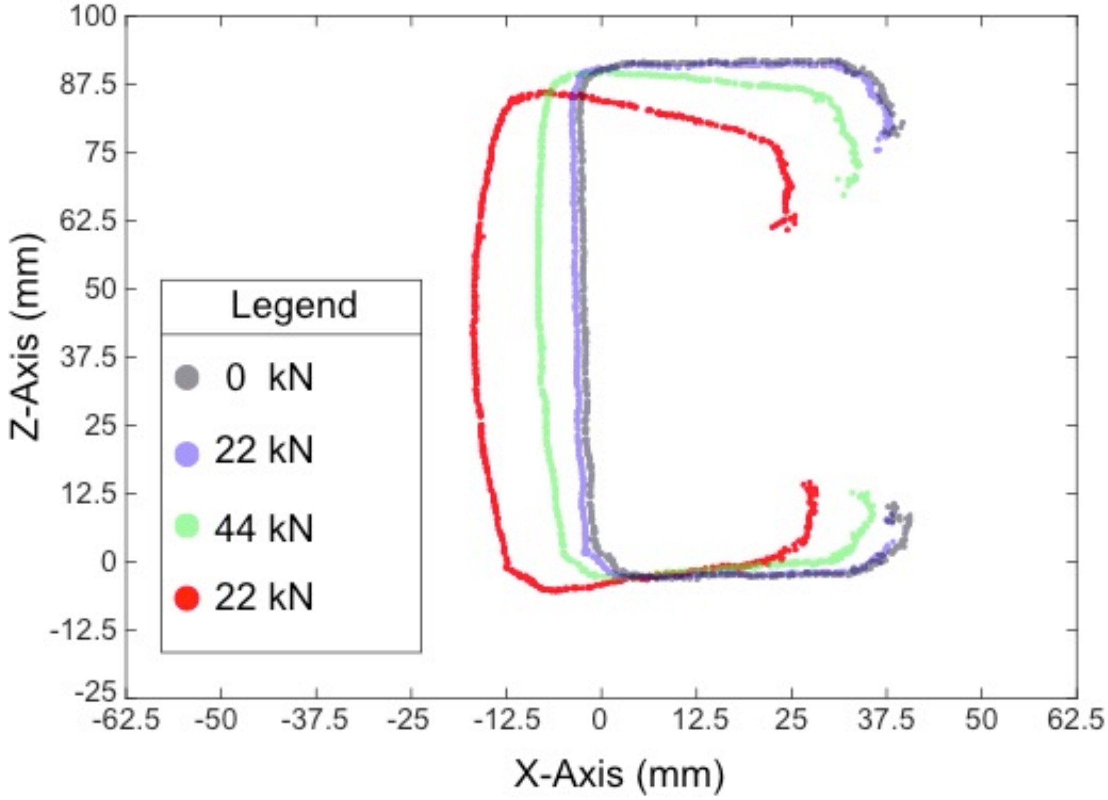

Figure 7: Specimen 2 cross-section deformation as function of axial load

To prepare for the modal identification procedure described in the following section, each of the specimen cross-sections was discretized into 9 nodes, segmenting the web and flanges as shown in Figure 8a. (Lip geometry was not accurately reconstructed and therefore they are not included in the discretization). Figure 8b shows a cross-section point cloud plot (points are in blue color), assuming they are all coplanar. The node discretization was fit into the outside boundary points of the cross-sections. The red line in Figure 8c represents the points detected as the boundaries of a cross-section point cloud and the orange line with yellow dots in Figure 8d represents the fitted node discretization and cross sectional elements. All the points that are not part of the section boundaries were considered noise and discarded.   The 200 cross-sections per specimen are used as input to a modal participation tool described in the following section.

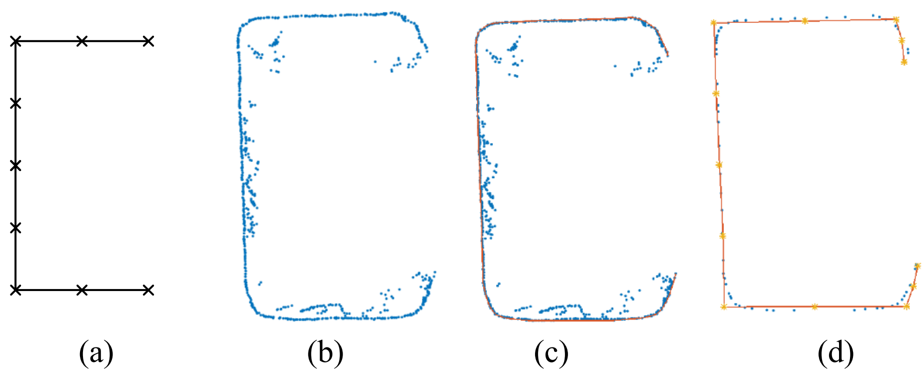

Figure 8: Cross-section (a) discretization for modal identification tool; (b) raw point cloud; (c) section boundary points; (d) automatic node fitting

6. Buckling mode participation using 3d point clouds and generalized beam theory

The cross-sectional dimensions and material properties of each specimen are inputted into a freely available tool Buckling Cracker (Cai 2014) and generalized beam theory (GBT) mode shapes of Specimen 1 are generated as shown in Figure 9 (Specimen 2 mode shapes are similar and not shown).

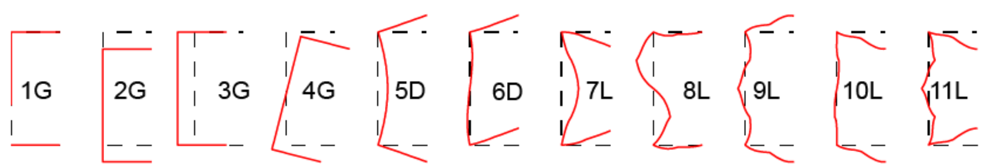

Figure 9: GBT mode shapes for Specimen 1, G global, D distortional, L local buckling

The displacement field at 200 cross-sections along each specimen is then used as input for GBT bucking mode identification. Buckling Cracker calculates the modal amplitudes and mode participation factors (Cai and Moen 2015). Relative participation of the dominant modes along the height of Specimens 1 and 2 are shown in Figures 10 and 11. The member modal participation factors are recorded in Tables 1 and 2. Note that the participation factor at 0 kN (initial imperfections) should be considered separately from the participation factors under load because the factors with load are calculated assuming the initial imperfection as the baseline geometry (i.e., with the initial imperfections removed).

For both Specimen 1 and Specimen 2, distortional and local buckling modes mix in the deformed shape up to peak load which is to be expected for this cross-section. Weak axis flexural buckling dominates after peak load as the flanges and web developed plastic folds and hinges. The modal participation results are consistent with observations during the experiments.

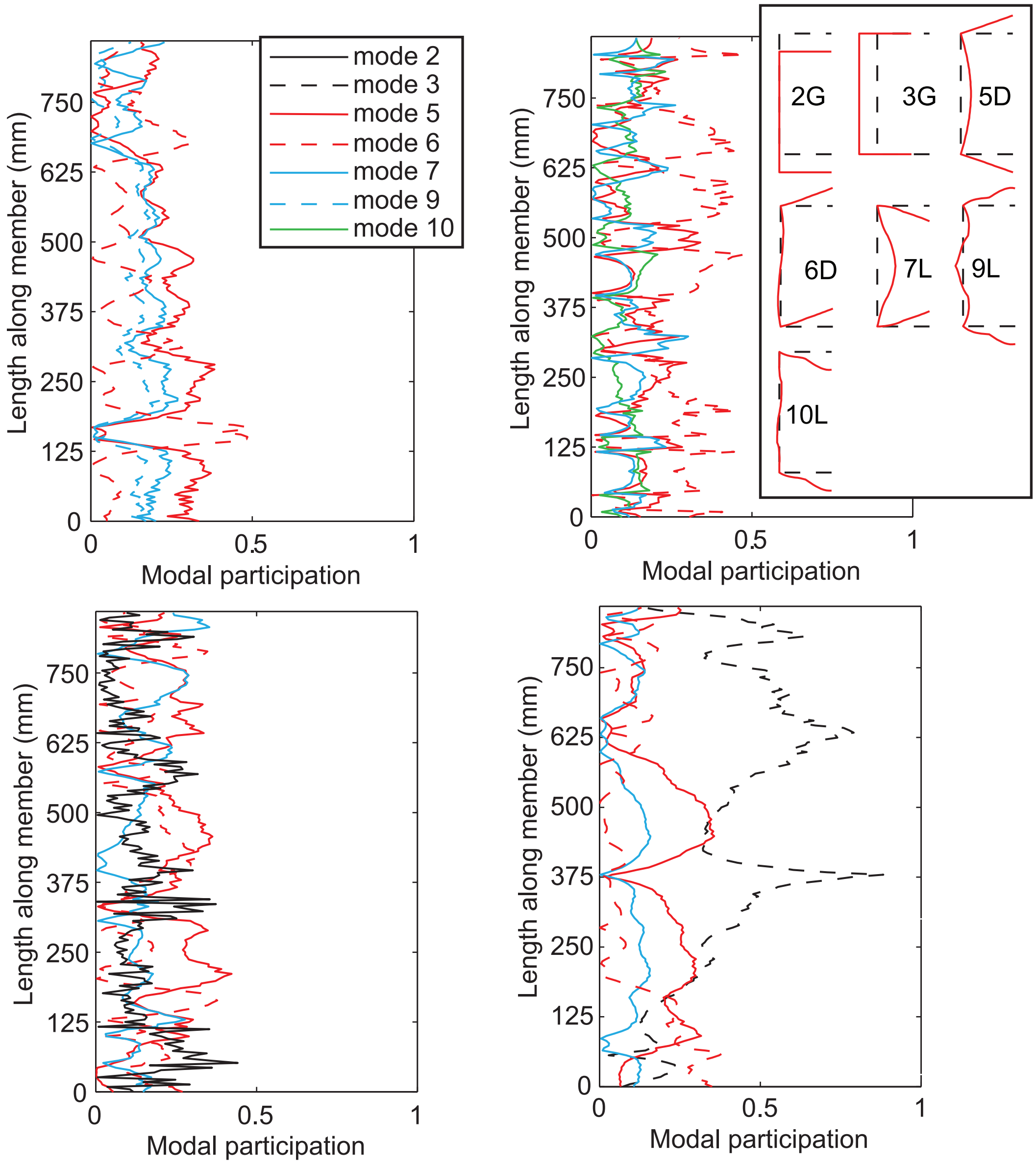

Figure 10: Specimen 1–cross-section modal amplitudes at load: (a) 0 kN (initial imp); (b) 22 kN; (c) 44kN;(d) 22 kN

Table 1: Specimen 1 –Member modal participations - G global, D distortional, L local buckling

Load (kN)	G	D	L
0 (imp.)	*0.24*	*0.34*	*0.42*
22	0.09	0.43	0.48
44	0.25	0.40	0.35
22	0.46	0.30	0.24

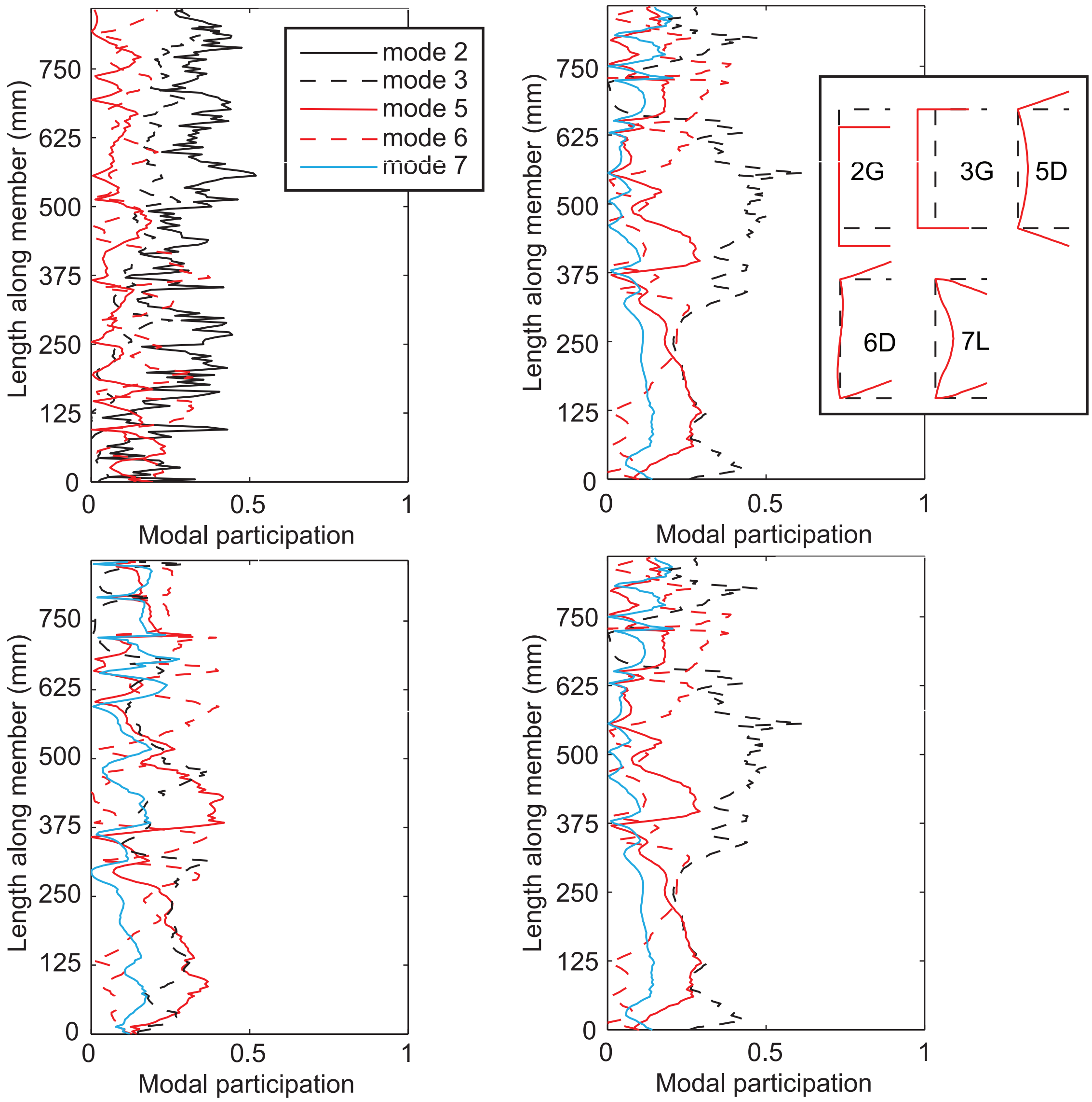

Figure 11: Specimen 2 - modal amplitudes at load: (a) 0 kN (initial imp.); (b) 22 kN; (c) 44kN; and (d) 22 kN

Table 2: Specimen 2 - Modal participations. G denotes global, D denotes distortional, L denotes local

Load (kN)	G	D	L
0 (imp.)	*0.51*	*0.23*	*0.26*
22	0.25	0.36	0.39
44	0.25	0.40	0.36
22	0.37	0.35	0.28

7. Conclusion

Off-the-shelf digital cameras and software were used to perform 3d image-based reconstruction of two cold-formed steel structural studs loaded to collapse in compression. Each image reconstructions were made up of approximately 30 million points. When scaled and aligned, the 3d point clouds were used to make cross-section measurements with an accuracy of ± 1 mm. The image reconstructions were used to measure initial geometric imperfections and to track cross-section deformation at column mid-height including distortional buckling and weak axis flexure deformation at peak load. Modal participation throughout the load-deformation response was also characterized. Research efforts are ongoing to establish formal reconstruction protocols including lighting and image quality to improve point cloud accuracy and consistency, especially at the flange stiffening lips which were the most challenging cross-section components to document.

Acknowledgements

The authors are grateful for the support of Virginia Tech PhD student Rafic G. El-Helou for helping with the experiments and specimen preparation and master's student Brandon Bowles for building the mold for the concrete end caps.

References

Cai, J. (2014). "Buckling Cracker. "http://www.moen.cee.vt.edu/category/tools/ and https://www.youtube.com/watch?v=kRsrmb1bWeI accessed Jan. 12, 2015.

Cai, J., Moen,C.D. (2015). "Automated Buckling Mode Identification of Thin-walled Structures from 3d Mode Shapes or Point Clouds." *Structural Stability Research Council Annual Conference*. USA, Nashville, TN.

Cheng, H.D., and Glazier C. (2002). "Automated Real-Time Pavement Crack Deflection/Classification System". Report NTIS # PB2003-101350, National Technical Information Service.

Crandall, D., Owens, A., Snavely, N., and Huttenlocher, D. (2011). "SfM with MRFs: discrete-continuous optimization for large-scale structure from motion". CVPR'11, pp. 3001– 3008.

Golparvar-Fard, M., Peña-Mora, F., Arboleda, C., and Lee, S. (2009). "Visualization of Construction Progress Monitoring with 4D Simulation Model Overlaid on Time-Lapsed Photographs." *J. Comput. Civ. Eng.* 23, SPECIAL ISSUE: Graphical 3D Visualization in Architecture, Engineering, and Construction, 391–404.

McAnallen, L., Zhao, X., Padilla-Llano, D., Moen, Cristopher, Eatherton, Matthew, Schafer, B. W. (2014). *Non-Contact Measurements and Characterization of Initial Geometric Imperfections in Cold-Formed Steel C-Section Structural Members*. Toronto: SSRC Annual Conference.

Perry, T. (2013). Agisoft's PhotoScan. Animation, 27(2), 38.

Tao, F., Salomon, A., Moen, C.D. (2015). "Experiments on cold-formed steel studs with concrete end supports." Virginia Tech Civil and Environmental Engineering Report SEM-15-01, Blacksburg, VA.

Torok, M. M., Golparvar-Fard, M., and Kochersberger, K. B. (2013). "Image-Based Automated 3D Crack Detection for Post-Disaster Building Assessment." Journal of Computing in Civil Engineering.

Wang, K.C.P. (October 2004)."Automated Pavement Distress Survey Through Stereovision". Report NTIS # PB2004-106775, National Technical Information Service.

Whelan, Matthew J., Ralston, Adam D., and Weggel,David C. (2015). "Blast Testing of Cold-Formed Steel Stud Wall Panels." *ASCE Journal of Performance of Constructed Facilities* (to appear).

Wu, C. (2011). "VisualSFM: A Visual Structure from Motion System – Documentation". <http://ccwu.me/vsfm/> accessed February 28, 2014.

Wu, C. (2013). "Towards Linear-Time Incremental Structure from Motion." 2013 International Conference on 3DV-Conference, 127–134.

Zheng, P., Moen, C.D. (2013). "Crack Detection and Measurement Utilizing Image-Based Reconstruction". Virginia Tech Civil and Environmental Engineering Report SEM-13-01, Blacksburg, VA.

Li, Z., Joó, A.L., Ádány, S., Schafer, B.W. (2011) "*Approximate modal identification in nonlinear collapse analysis of thin-walled members.*" Structural Stability Research Council - Proceedings of the 2011 Annual Stability Conference, Pittsburg, PA, USA; May 10-14.